# In Situ X-Ray Reflectivity and Voltammetry Study of Ru(0001) Surface Oxidation in Electrolyte Solutions

## J. X. Wang,[†] N. S. Marinković,[†] H. Zajonz,[‡] B. M. Ocko,[‡] and R. R. Adžić*,[†]

*Materials and Chemical Sciences Division, Energy Sciences and Technology Department, Building 555, and Department of Physics, Brookhaven National Laboratory, Upton, New York 11973*

*Received: November 13, 2000*

The electrochemical surface oxidation of Ru(0001) in acid solutions is limited to a one-electron process resulting in one monolayer oxygen uptake at potentials below the onset of bulk oxidation at 1.35 V. In 1 M $H_2SO_4$, about $^1/_3$ monolayer of bisulfate anions are coadsorbed with hydronium cations at low potentials. The spacing between the top two Ru layers is 2.13 Å at 0.1 V and 2.20 Å at 1.0 V, similar to those found in the gas phase for bare Ru (2.10 Å) and for one monolayer of oxygen on Ru (2.22 Å), respectively. In contrast to Pt(111) and Au(111) surfaces, no place exchange is involved in the Ru(0001) surface oxidation. On the oxidized surface, the oxygen species stays on top of a smooth ruthenium surface causing a partial desorption of the bisulfate ions. The lack of subsurface oxygen on a Ru(0001) electrode is postulated to be the origin of its inactivity for CO oxidation found in a separate study.

## I. Introduction

Ruthenium oxidation has been the subject of extensive research because of the specific catalytic properties of ruthenium oxides. Ruthenium is an important cocatalyst material in Pt−Ru fuel cell electrocatalysts for methanol and reformate hydrogen oxidation;[1−2] ruthenium oxide is a component in chlorine evolution catalysts,[3] and it represents an attractive material for electrochemical supercapacitors.[4] The electrooxidation of polycrystalline ruthenium has been investigated by a variety of techniques.[5−12] The work with electrodeposited Ru[5] and bulk polycrystalline Ru[6,7] revealed pronounced differences in hydrogen adsorption and surface oxidation of these two materials. Hydrogen adsorption and multilayer-oxide formation are more facile at electrodeposited Ru surfaces. Vibrational properties of Ru oxides have been studied by surface enhanced Raman spectroscopy,[8] and reflectance spectroscopy was used to identify soluble higher valency ruthenium species.[9] Impedance techniques provided an additional characterization of a high capacitance behavior and kinetics of proton-transfer reactions,[10,11] whereas ellipsometry was used to determine the oxide layer thickness, as well as some optical and structural properties.[12]

Recent activities in the development of fuel cell technology have renewed efforts to improve Pt−Ru electrocatalysts. In bifunctional Pt−Ru electrocatalysts, it has been conjectured that Ru provides active oxygen so that CO, a poison species for the surface catalytic reactions, can be oxidized and removed at potentials lower than those observed for Pt.[13] To gain an atomic level understanding of the catalytic property, studies of single-crystal surfaces are desirable. A pronounced structural sensitivity has been demonstrated for several reactions on Ru surfaces.[14−19] For example, bisulfate adsorption was observed by in situ Fourier transform infrared spectroscopy (FTIR) on Ru(0001), but not on polycrystalline surface.[18] Carbon monoxide is unusually stable on a Ru(0001) electrode surface, in sharp contrast with the facile electrooxidation on a polycrystalline surface.[15,17] CO adsorbs on Ru(0001) in linear and 3-fold bonding configurations, whereas only a linear configuration has been observed on polycrystalline surfaces. This indicates that the adsorption configuration does not determine the reactivity of CO on Ru, otherwise linear CO should be oxidized on Ru-(0001) as it is on polycrystalline surfaces. Clearly, other factors, such as the presence of active oxygen at the surface, are more important, giving an additional incentive for studies of the surface oxidation on Ru single-crystal electrodes.

The oxidation of Ru single crystal surfaces has been extensively studied from the gas phase.[20] For example, the exposure of Ru(0001) to low pressure of $O_2$ facilitates the formation of a $(2 \times 2)$-O and a $(2 \times 1)$-O superstructures with O-coverages (defined with respect to the atomic density of the Ru(0001) surface) of 0.25 and 0.5, respectively.[21] By exposing the Ru(0001) surface either to large amount of $O_2$, or alternatively by using dissociative $NO_2$ chemisorption at elevated sample temperature, the $(2 \times 2)$-3O phase (coverage of 0.75) and an on-surface $(2 \times 1)$-O monolayer can be formed with a negligible amount of subsurface oxygen (i.e., between the first two Ru layers).[22] In addition, the spacing between the first two Ru layers has been found to increase as the oxygen coverage is increased from zero to one monolayer. More recently, the relationship between the formation of the subsurface oxygen phase and the growth of oxides during oxidation of Ru(0001) was determined[23] and correlated with the catalytic activity of ruthenium for the CO oxidation reaction.[24] $RuO_2$ grows epitaxially at elevated sample temperature (600−800 K) in the presence of a large amount of molecular oxygen on the Ru(0001) and the Ru(10$\bar{1}$0) surfaces with its (110) and (100) faces oriented parallel to the substrate surface, respectively.[25,16] In contrast, ex situ UHV-electrochemical study shows that the oxidation at high potentials results in $RuO_2$ epitaxial growth with its (100) plane parallel to the Ru(0001) surface.[16]

* To whom correspondence should be addressed. Fax: 631 344-5815. E-mail: adzic@bnl.gov.
† Materials and Chemical Sciences Division, Energy Sciences and Technology Department, Brookhaven National Laboratory.
‡ Department of Physics, Brookhaven National Laboratory.

The present in situ structural study focuses on the initial stage of electrochemical oxidation at potentials negative of the bulk oxidation. Although surface X-ray scattering techniques are not directly sensitive to the valency state of the surface atoms, it has been demonstrated that important insights can be gained from the correlation between the change of surface structure and the current behavior. For example, H. You et al.[26] have confirmed by using in situ X-ray techniques that the place-exchange occurs in the Pt(111) surface oxidation. For Ru(0001), we found a very different structural phase behavior. The results will be compared with gas-phase oxidation phase behavior, and the implications for the catalytic properties of Ru will be discussed.

## II. Experimental Aspects

The Ru(0001) crystal (9 mm in diameter) was obtained from Metal Crystals and Oxides, Cambridge, England. The miscut from the (0001) face was corrected to be better than 0.1°. The surface preparation was performed in ultrahigh vacuum (UHV) following the standard procedure:[21] sputtering at room temperature with 1 keV Ar ions, followed by five cycles of oxygen adsorption/desorption to remove carbon and a final flash annealing in UHV at 1400 °C to remove the residual oxygen. After cooling in a vacuum, the crystal was transferred through an Ar-filled glovebox into an electrolyte solution. Protected by the solution drop or by adsorbed CO (which was desorbed in the first oxidation cycle), the crystal was then mounted into a X-ray or regular electrochemical cell. The bulk mosaic width was 0.05° and the full width at half-maximum (fwhm) of the $\theta$-rocking curve near the anti-Bragg positions was about 0.15°. The same surface preparation procedure was used for the polycrystalline Ru electrode in electrochemical experiments. This allows attribution of the differences in voltammograms to the differences in atomic structure between the two surfaces.

The solutions were prepared from Optima* sulfric and perchloric acids from Fisher and Milli-QC UV−Plus water (Millipore Inc.) and kept free from oxygen during the X-ray and electrochemical measurements. Potentials were measured against a reversible hydrogen electrode (RHE) or a Ag/AgCl-(3M NaCl) electrode. All potentials in this article are given with respect to RHE. All of the voltammetry curves shown were obtained with a hanging meniscus configuration.

X-ray measurements were performed at beam line ×22A with $\lambda = 1.20$ Å at the National Synchrotron Light Source. Following convention, a hexagonal coordinate system was used for the Ru(0001) crystal in which the reciprocal-space wave vector was $Q = |H\vec{a}^* + K\vec{b}^* + L\vec{c}^*|$, where $a^* = b^* = 4\pi/\sqrt{3}a(a = 2.706$ Å$)$, $c^* = 2\pi/c$, $c = 4.282$ Å$)$, and $L$ is along the surface normal direction. Specular reflectivity profiles were measured with a $2 \times 2$ mm slit located 650 mm from the sample. The resulting resolution in the surface plane was 0.01 Å$^{-1}$ (fwhm), which is larger than the intrinsic peak width for all measured reflections.

## III. Results and Discussion

**A. Voltammetry of Ru(0001) Surface Oxidation.** Figure 1 shows the voltammetry curves for the surface oxidation of Ru(0001) in three acidic solutions containing different anions. The negative potential limits were carefully chosen to avoid the complications associated with hydrogen adsorption/evolution near 0 V versus RHE. Before starting a cycle in the positive direction, the potential was held at the negative limit long enough to ensure the reduction current originating from the previous potential cycle was negligible. In all three solutions,
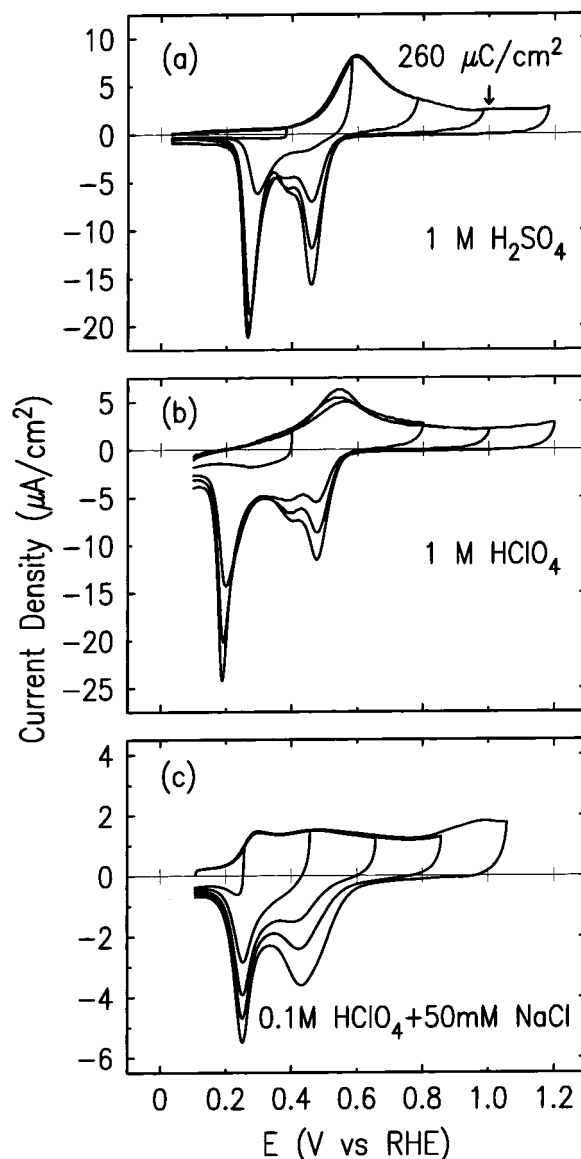


**Figure 1.** Voltammetry curves for Ru(0001) surface oxidation with different positive potential limits in acidic solutions containing different anions. Sweep rate = 10 mV/s.

the voltammerty curves show a single anodic peak with a long tail extending to the onset of bulk oxidation and two major cathodic peaks correlated to the reduction processes which initiate at 0.6 V for all three curves.

In 1 M $H_2SO_4$ (Figure 1a), the surface oxidation occurs above 0.4 V and the integrated anodic charge reaches 260 $\mu$C/cm$^2$ in the sweep up to 1 V. This is equivalent to the charge for a one-electron oxidation of the Ru(0001) surface. The net charge obtained by integrating the current for a whole potential cycle is close to zero. Increasing the sweep rate results in a linear increase in the current density for sweep rates up to 500 mV/s. Repeated potential cycling between 0 and 1.2 V did not cause significant change in the voltammetry curves. All these facts suggest that the Ru(0001) surface oxidation is limited to the top layer with one electron per atom exchange at the potential below the onset of bulk oxidation.

In 1 M $HClO_4$ (Figure 1b), the anodic current gradually rises from the beginning of the potential cycle, and the integrated charge between 0.1 and 1 V is 230 $\mu$C/cm$^2$, slightly less than that required for a one-electron surface oxidation process. In the negative potential sweep, the onset of reduction and the

Ru(0001) Surface Oxidation in Electrolyte Solutions

*J. Phys. Chem. B, Vol. 105, No. 14, 2001* **2811**

potential of the first cathodic current peak are about the same as in the $H_2SO_4$ solution. However, the second major cathodic peak shifts negatively and a sizable cathodic current decays slowly after the potential cycle has ended. These features indicate that the reduction process cannot be completed in $HClO_4$ solution without extending the sweep into the hydrogen adsorption/evolution region. Why does bisulfate/sulfate adsorption affects the surface redox reaction at low potentials? Our FTIR and X-ray studies show that the bisulfate adsorption on Ru(0001) is essentially at a saturation coverage between 0 and 0.5 V and that water chemisorbs on Ru(0001) in the absence of chemisorbed anions. These facts suggest that strongly adsorbed bisulfate ions prevent water-induced oxygen adsorption processes at low potentials and promote the complete removal of the oxygen adsorbates in the cathodic sweep.

To further explore anion effects on the electrooxidation of Ru(0001), $Cl^-$ and $Br^-$ were added to the 0.1 M $HClO_4$ solution. The results in $Cl^-$ containing solution are shown in Figure 1c (data in the $Br^-$ solution are nearly identical and are not shown). A sharp rise of anodic current occurs near 0.2 V, which is at a more negative potential than the onset of surface oxidation in sulfuric acid. This shows that strongly adsorbed halide ions do not provide better protection for the Ru from surface oxidation than bisulfate ions. In the halide cases, it is likely that a different redox process occurs because they make compounds with ruthenium in several different oxidation states.

Figure 2a and 2b shows the voltammetry curves obtained after extending the negative potential limit to −0.1 V versus RHE in 1 and 0.1 M $HClO_4$ solutions. The increase of cathodic current below 0 V is due to hydrogen evolution. Although the voltammetry curve changes only slightly in the 1 M solution, an additional anodic peak appears near 0.26 V in the 0.1 M solution. The charge under this peak increases with increasing cathodic charge at potential below 0 V. Similar trends as a function of pH in this potential region have been reported in earlier studies,[14] including a strong peak in a pH = 3 solution and a small peak in a pH = 0 solution. In the voltammetry curves for Ru(0001) in 0.1 M $HClO_4$ solution reported by Lin et al.,[16] there is a pair of current peaks at potentials close to hydrogen evolution which were ascribed to the hydrogen adsorption process. We noticed similar feature after several potential sweeps into hydrogen evolution. This feature is strongly dependent on the potential cycling history.

In alkaline solution (pH = 14), the feature at low potentials is more striking. As shown in Figure 2c (solid line), a strong anodic current peak occurs at 0.36 V with an integrated charge corresponding to 1.2 $e^-$/atom, and a strong cathodic current peak occurs at 0.16 V with a charge equivalent to 1.4 $e^-$/atom. However, the integrated anodic charge from 0.4 to 1.0 V remained equivalent to 1 $e^-$/atom as in acid solutions. Extending the negative potential limit into the hydrogen evolution regime (dot−dash line) causes a slight potential shift and an increase of the anodic current peak. It appears that the Ru surface oxidation/reduction becomes more interwined with hydrogen adsorption/evolution as the pH increases. On polycrystalline Ru, the symmetric peaks in this potential range have been attributed to either hydrogen adsorption[27] or Ru oxidation.[28]

Finally, Figure 3a shows the onset of Ru(0001) bulk oxidation/dissolution and its effect on the voltammetry feature. After a few cycles involving the large anodic current near 1.35 V, the onset of surface oxidation, as well as the second reduction peak, shift to slightly more negative potentials (solid line) than those obtained previously (dashed line). Repeated cycling over a few hours did not cause significant additional changes in the
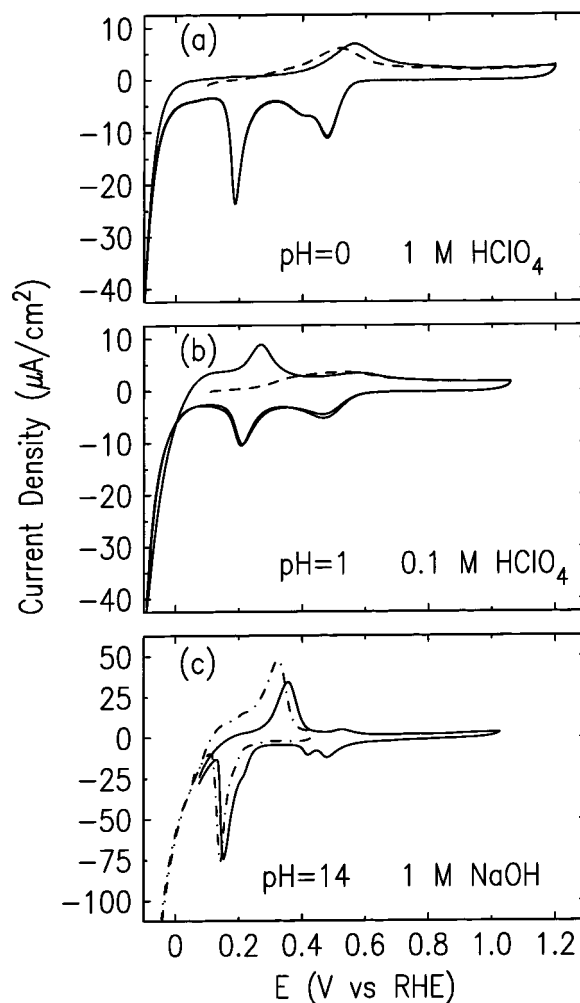


**Figure 2.** Voltammetry curves showing the effect of hydrogen evolution to the voltammetry of Ru(0001) surface oxidation in solutions of different pH. Sweep rate = 10 mV/s. Dashed line shows the first positive sweep started at potential positive of 0 V, which upon completion is followed by a potential cycle with a new low potential limit (solid line).

voltammetry curve. This behavior is very different from the potential-cycling induced oxide growth observed on Ru foil.[6] On a UHV-prepared polycrystalline Ru surface, as shown in Figure 3b, the voltammogram is featureless over the entire potential region, and the currents are about one order of magnitude higher than those on Ru(0001). These features suggest a high degree oxidation occurring continuously over a wide potential region on polycrystalline Ru. Such a large difference between the two surfaces is striking and demonstrates that Ru surface oxidation is highly structure sensitive.

**B. Surface X-ray Scattering.** To characterize the atomic structure of the Ru(0001) electrode as a function of potential, X-ray specular reflectivity profiles were measured at 0.1 and 1.0 V in 1 M $H_2SO_4$. In Figure 4, the structure factor intensities are shown after correcting the integrated intensities for the variation of the Lorentz factor, the effective sample area, and the resolution along the surface normal direction.[29] In comparison with the calculated curve for an ideally terminated Ru(0001) surface (dot and dash line), the measured specular reflectivities at 0.1 and 1.0 V have deeper minima. Simulations indicate that this could result from either adsorptions or changes in the top layer of the substrate. In sulfuric acid solutions, adsorbates can be sulfate ($SO_4^{2-}$) or bisulfate ($HSO_4^-$), and oxygen-containing species($H_3O^+$, $H_2O$, $OH^-$, and $O^{2-}$). Because the $H^+$ ion has
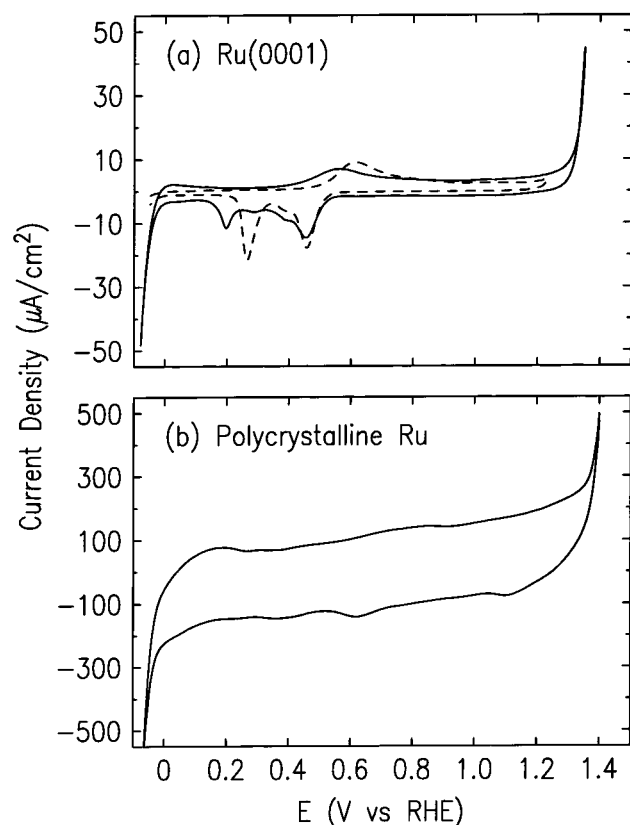
**Figure 3.** Voltammetry curves for Ru(0001) (a) and polycrystalline Ru (b) in 1 M $H_2SO_4$. Sweep rate = 10 mV/s.



**Figure 4.** Upper panel: Specular reflectivity (structure factor squared) measured for Ru(0001) at 0.1 V (circles) and 1.0 V (plus sign) in 1 M $H_2SO_4$ with the dot–dash line showing the calculated curve for an ideally terminated Ru(0001). The dashed and solid lines are the fits discussed in the text. Lower panel: Proposed structural models where the O, S, and Ru atoms are represented by the open, heavily shaded, and lightly shaded circles, respectively. The layer spacings are given in Å and coverages are given in monolayer (ML).

no electron and hence no contribution to the X-ray scattering cross section, specular reflectivity measurements cannot distinguish between sulfate and bisulfate and among the four oxygen-containing species because these species only differ in the number of $H^+$. To model the reflectivity, we allowed for two different adlayers. One contains only $O^{2-}$, which corresponds to the four possible oxygen-containing species and the other, containing one $S^{6+}$ and four $O^{2-}$, represents sulfate or bisulfate. In the following discussion, bisulfate will be considered as the sulfur-containing adsorbate on the basis of the identification made by our FTIR study.[18] For the oxygen-containing species, $H_3O^+$ cations and $OH^-$ anions are assumed to be the adsorbates at low (0.1 V) and high (1.0 V) potentials, respectively.

For the specular reflectivity at 0.1 V (circles), our first approach was to include only a bisulfate adlayer on the Ru-(0001) surface. To minimize the number of free parameters in the fitting process, we have assumed that the three coplanar oxygen atoms are 0.69 Å below the sulfur atom and the other oxygen atom is 1.55 Å above the sulfur atom, based on the bond lengths found for the Cu-sulfate coadsorption on Au-(111).[30] The free parameters in the fitting are the bisulfate coverage, the layer spacing between the three coplanar oxygen atoms and the top Ru layer, the root-mean-square (RMS) displacement amplitude (Debye–Waller factor) for the atoms in the bisulfate adlayer, the spacing between the top two Ru layers, and the RMS displacement amplitude for the top Ru layer. The best fit is shown by the dashed line in Figure 4, which gives a 0.4 monolayer of bisulfate and a nearly ideally terminated Ru(0001) crystal.

An improved description of the data was obtained by adding an oxygen adlayer in the model. The best fit (solid line) gives a 2.13 ± 0.01 Å spacing between the top two Ru layers and a RMS displacement amplitude of 0.13 ± 0.02 Å for the top Ru
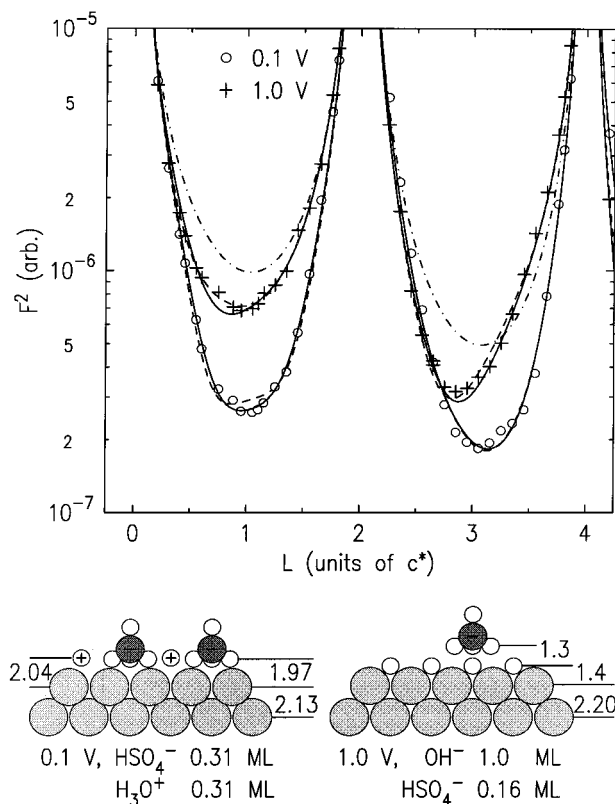
layer. Compared to the fit without oxygen, the bisulfate coverage decreased from 0.40 to 0.31 ± 0.05, whereas the layer spacing between the coplanar oxygen atoms and the top Ru layer remained at 1.97 ± 0.05 Å. The oxygen adlayer was found to have the same coverage (0.31 ± 0.05) as the bisulfate adlayer with a Ru–O layer spacing of 2.04 ± 0.21 Å. Despite differences in the adlayer, both models indicate that the Ru-(0001) surface is nearly ideally terminated. The saturated coverage for bisulfate is expected to be about $^1/_3$ or 0.4 monolayer based on its size relative to the Ru(0001) surface. On Pt(111), the bisulfate coverage increases with increasing potential and reaches the saturation at rather high potentials.[31] Can a high-coverage bisulfate adsorption on Ru(0001) at 0.1 V be justified? To answer this question and to understand the nature of the oxygen-containing adsorbate, we measured X-ray specular reflectivity for Ru(0001) in pure water.

The specular reflectivity curve obtained from Ru(0001) in pure water (not shown) has deeper minima compared to the curve for an adsorbate-free Ru(0001), and we attribute this feature to water adsorption. The analysis suggests a monolayer of water or oxygen on Ru(0001) with a 2.03 ± 0.05 Å Ru–O layer spacing. This spacing is close to the Ru–O bond length for the gas-phase adsorbed oxygen but much smaller than the 3 Å layer spacing for water adsorption on Au(111)[32] and on Ag(111).[33] These facts suggest that water is chemisorbed on Ru(0001). In addition, the spacing between the top two Ru layers is 2.17 Å, larger than 2.13 Å found in sulfuric acid at 0.1 V. For gas-phase oxidation, this layer spacing expands from 2.10 to 2.22 Å as the oxygen coverage increases from 0 to 1 mono-

layer.[22] Thus, the expansion of Ru layer spacing in pure water suggests that the water adsorption involves an oxidation process. On the other hand, the smaller Ru layer spacing in sulfric acid solution at low potentials indicates that the oxidative water adsorption is circumvented by the adsorption of bisulfate. In 1 M strong acid solution at low potentials, the coadsorbed oxygen species is likely to be the hydronium ion ($H_3O^+$). As illustrated by the model in the bottom panel of Figure 4, the two adlayers are nearly coplanar. The lateral electrostatic repulsion among the bisulfate anions can be reduced by the coadsorption of $H_3O^+$ cations. This kind of cation−anion coadsorption usually results in a constant coverage over a range of potentials,[34,35] and thus, the high bisulfate coverage is reached at a very low potential. Another case for sulfate/bisulfate adsorption over a wide potential region has been reported for the Rh(111) surface.[36]

At potentials positive of the anodic current peak, a partial desorption of bisulfate has been observed by FTIR,[18] which is believed to be a result of the formation of a surface oxide. This is confirmed by the analysis of the specular reflectivity obtained at 1.0 V shown by the plus symbol in Figure 4. The most clear evidence for that is the $2.20 \pm 0.02$ Å spacing between the top two Ru layers, which was found independent of the details on the adlayer structure and similar to the value (2.22 Å) for one monolayer of oxygen on Ru(0001) in gas-phase oxidation.[22] For the oxygen and bisulfate adlayers, the fitting parameters are strongly correlated. The dashed line shows the best fit when the spacing between the oxygen layer and the top Ru layer was initially fixed at 1.5 Å. It gives 1.0 monolayer of oxygen located at 1.6 Å above the top Ru surface and 0.08 monolayer of bisulfate at 1.9 Å above the oxygen layer. The solid line was obtained by fitting with the spacing between the oxygen layer and the top Ru layer initially fixed at about 1 Å. This fit gives 0.8 monolayer of oxygen located at 1.2 Å above Ru, and 0.24 monolayer of bisulfate located at 0.7 Å above the oxygen layer. Alternatively, fitting with the oxygen layer located under the top Ru layer failed to yield a reasonable good fit and, on this basis, we can rule out the existence of subsurface oxygen. On the basis of these results, a structural model is proposed as described by the lower panel of Figure 4 (right side half). Although the parameters given for the adsorbates (average values from two sets of parameters) have large error bars, the results do support the formation of surface oxide and suggest that a monolayer of oxygen species is chemisorbed and stays on top of the Ru(0001) surface at 1.0 V. This, in turn, results in a partial desorption of bisulfate.

To gain further insight into the potential-induced phase transition at the Ru(0001) electrode surface, the X-ray intensities at the (0,0,1.1) and (0,0,2.5) positions were monitored whereas sweeping the potential between 0 and 1.2 V at 1 mV/s. Figure 5 shows these potential-dependent intensities together with the voltammetry curve obtained at the same sweep rate, albeit in a separate cell. Although both the bisulfate desorption and the layer expansion of the Ru surface contribute to the intensity increase at the (0,0,1.1) position at high potentials, the later has a dominant and opposite effect on the X-ray intensity at (0,0,2.5). As shown in the top panel of Figure 5, the (0,0,1.1) intensity is constant up to 0.57 V in the positive potential sweep suggesting no significant change in either Ru surface or adlayer coverage below this critical potential, even though the anodic current starts to rise at a slightly more negative potential. Above 0.57 V, the (0,0,1.1) intensity continuously increases with increasing potential, which is accompanied by the intensity decrease at the (0,0,2.5) position. This confirms that an electrooxidation-induced surface expansion occurs on Ru(0001),
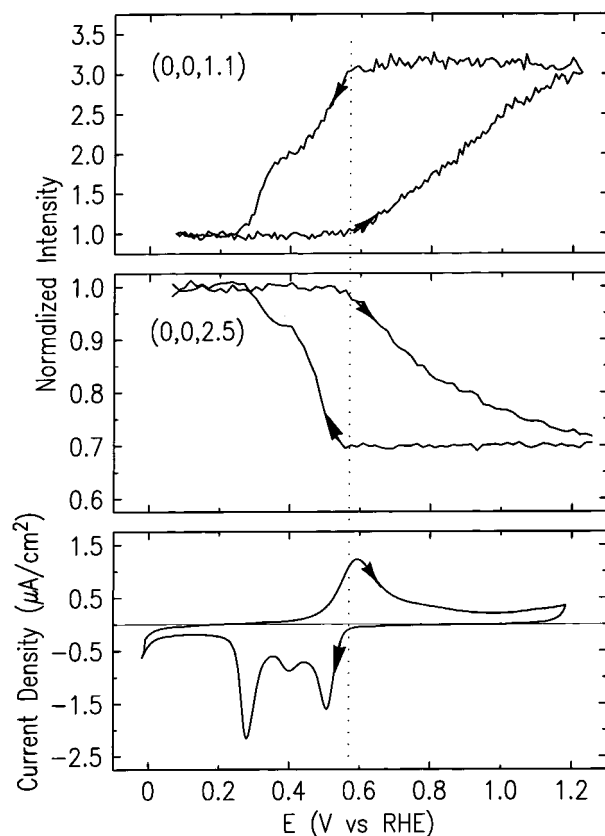


**Figure 5.** X-ray intensities as a function of potential and the corresponding voltammetry curve for Ru(0001) in 1 M $H_2SO_4$. Sweep rate = 1 mV/s. The X-ray intensities measured at the (0,0,1.1) and (0,0,2.5) positions are shown after subtracting the diffuse scattering background and normalizing the intensities at the most negative potentials to unity. The vertical dotted line highlights the critical potential (0.57 V) where the onset of structural changes due to the surface oxidation/reduction occurs.

above this critical potential. After the potential sweep reversal, both X-ray intensities remain constant over the entire oxide-formation potential region down to 0.57 V. At this critial potential, the onset of oxide reduction occurs, which is apparent from the voltammetry curves. This is followed immediately by the inversed structural phase transition as indicated by the changes in the (0,0,1.1) and (0,0,2.5) intensities. The steep slopes in the X-ray intensity curves correlate well with the reduction current peaks. In repeated potential cycles, the X-ray intensities do not vary with the number of cycles, indicating no irreversible roughening and no progressive oxide formation, in agreement with the conclusion based on the voltammetry measurements.

Ordered (2 × 2), (3 × 1), and (1 × 1) oxygen adlayers have been identified in UHV by low-energy electron diffraction (LEED) and Auger electron spectroscopy (AES) on the Ru-(0001) electrode emersed from 0.1 M $HClO_4$ solution at potentials close to 0.4, 0.6, and 1.2 V (vs RHE), respectively.[16] In our experiments for Ru(0001) in sulfuric acid, no in-plane diffraction features can be correlated to these ordered submono-layer oxygen phases. We note that the expected X-ray intensity from an oxygen adlayer is weak relative to the diffuse scattering background originating from the thin solution layer and the plastic film. Thus, from the absence of superlattice peaks, it is difficult to rule out the existence of these ordered structures. However, there is also no indirect evidence to support these submonolayer oxygen phases in sulfuric acid from the specular reflectivity measurements. Nevertheless, both the in situ X-ray and the ex situ LEED and AES studies show that the initial

**2814** *J. Phys. Chem. B, Vol. 105, No. 14, 2001*

Wang et al.

state of Ru(0001) oxidation involves oxygen adsorption of up to one full monolayer at potentials below the onset of Ru bulk oxidation in acid solutions.

The structural phase behavior of Ru surface oxidation is distinctly different from those observed for other noble metal surfaces. For Pt(111), as demonstrated by X-ray reflectivity studies, the electrochemical surface oxidation involves a place exchange where a fraction of the top Pt atoms moved on top of the original surface layer forming partially filled Pt layers.[26] On Au(111), the place exchange occurs in the potential region of the second surface oxidation current peak.[37] When these partially filled layers form at the substrate surface, a sharp decrease of intensity occurs near the anti-Bragg positions. This feature is absent for Ru(0001) at potentials below 1.2 V. In fact, due to the desorption of bisulfate, an increase of the X-ray intensity near the anti-Bragg positions was observed upon the oxide formation. Therefore, it is unambiguous that place exchange is not involved in the Ru(0001) surface oxidation.

## IV. Summary

The electrochemical surface oxidation of Ru(0001) has been characterized by means of in situ surface X-ray scattering techniques and cyclic voltammetry. In acid solutions, the voltammetry curves show a one-electron surface oxidation process at potentials below the onset of bulk oxidation. Furthermore, the analysis of the X-ray specular reflectivity found that the spacing between the top two Ru layers is 2.13 Å at 0.1 V and 2.20 Å at 1.0 V in 1 M sulfuric acid solution, similar to those found in gas phase for bare Ru (2.10 Å) and for one monolayer of oxygen on Ru (2.22 Å), respectively. At low potentials, specular reflectivity data support a model involving the coadsorption of bisulfate and hydronium ions on Ru(0001). The coverage of bisulfate is close to $^1/_3$ monolayer at potentials below the phase transition potential of 0.57 V. In contrast to the behavior of Pt(111) and Au(111) surfaces, no place exchange is involved in the Ru(0001) surface oxidation. The formation of a monolayer of ruthenium oxide causes a partial desorption of bisulfate in agreement with the FTIR results.[18] It is striking that oxygen penetration is completely blocked on Ru(0001) at potentials below the bulk oxidation potential in contrast to the high degree surface oxidation of polycrystalline Ru, which occurs between the onset of hydrogen evolution to the onset of bulk oxidation. Because it is known from gas-phase studies that the subsurface oxygen plays a major role in the catalytic activity of Ru for CO oxidation,[24] the lack of subsurface oxygen on the Ru(0001) electrode is a possible explanation for its inactivity for CO electrooxidation found in.[15]

## References and Notes

(1) Landgrebe, A. R., Sen, R. K., Wheeler, D. J., Eds.; *DOE Workshop on Direct Methanol Oxidation Fuel Cells*; Proc. Vol. 92, The Electrochemical Society: Pennington, New Jersey, 1992.

(2) Gasteiger, H. A.; Markovic, N.; Ross, P. N.; Cairns, E. J. *J. Phys. Chem.* **1993**, *97*, 12 020.

(3) Trasatti, S.; O'Grady, W. E. In *Advances in Electrochemistry and Electrochemical Engineering*; Gerisher, H., Tobias, C., Eds.; J. Wiley: New York, 1982; Vol. 12.

(4) Conway, B. E. *Electrochemical Supercapacitors: Scientific Foundations and Technological Applications*; Kluwer Academic/Plenum Publishers: New York, 1999.

(5) Hadzi-Jordanov, S.; Angerstein-Kozlowska, H.; Vukovic, M.; Conway, B. E. *J. Electrochem. Soc.* **1978**, *125*, 1569.

(6) Michell, D.; Rand, D. A. J.; Woods, R. *J. Electroanal. Chem.* **1978**, *89*, 11.

(7) Lezna, R. O.; De Tacconi, N. R.; Arvia, A. *J. Electroanal. Chem.* **1983**, *151*, 193.

(8) Chan, H. Y. H.; Takoudis, Ch. G.; Weaver, M. J. *J. Catal.* **1997**, *172*, 336.

(9) Walker, R. C.; Baisiles, M.; Peter, L. M. *Electrochim. Acta* **1998**, *44*, 1289.

(10) Ripshon, J.; Gottefeld, Sh. *J. Electrochem. Soc.* **1984**, *131*, 1960.

(11) Horvat-Radosević, V.; Kvastek, K.; Vuković, M.; Čukman, D. *J. Electroanal. Chem.* **2000**, *482*, 188.

(12) Velikodnii, L. N.; Shefelin, V. A.; Kasatkin, E. V. *Elektrohimiya* **1982**, *7*, 1275.

(13) Herrero, E.; Franaszczuk, K.; Wieckowski, A. *J. Electroanal. Chem.* **1993**, *361*, 269. (b) Chrzanowski, W.; Wieckowski, A. *Langmuir* **1997**, *13*, 5974.

(14) Cao, E. Y.; Stern, D. A.; Gui, J. Y.; Hubbard, A. T. *J. Electroanal. Chem.* **1993**, *354*, 71.

(15) Marinković, N. S.; Zajonz, H.; Adžić, R. R. *195th Electrochem. Soc. Meeting, Book of Abstracts*; p1044, Seatle, WA 1999. (b) Marinković, N. S.; Wang, J. X.; Zajonz, H.; Adžić, R. R. *Electrochem. Solid-State Lett.* **2000**, *3*, 508.

(16) Lin, W. F.; Zei, M. S.; Kim, Y. D.; Over, H.; Ertl, G. *J. Phys. Chem. B* **2000**, *104*, 6040.

(17) Lin, W. F.; Christensen, P. A.; Hamnett, A.; Zei, M. S.; Ertl, G. *J. Phys. Chem. B* **2000**, *104*, 6642.

(18) Marinković, N. S.; Wang, J. X.; Zajonz, H.; Adžić, R. R. *J. Electroanal. Chem.*, in press.

(19) Ikemiya, N.; Senna, T.; Ito, M. *Surf. Sci.* **2000**, *464*, L681.

(20) Over, H. *Prog. Surf. Sci.* **1998**, *58*, 249, and references therein.

(21) Madey, T. E.; Engelhardt, H. A.; Menzel, D. *Surf. Sci.* **1975**, *48*, 304.

(22) Stampfl, C.; Schwegmann, S.; Over, H.; Scheffler, M.; Ertl, G. *Phys. Rev. Lett.* **1996**, *77*, 3371. (b) Kim, Y. D.; Wendt, S.; Schwegmann, S.; Over, H.; Ertl, G. *Surf. Sci.* **1998**, *418*, 267.

(23) Bottcher, A.; Niehus, H. *J. Chem. Phys.* **1999**, *110*, 3186.

(24) Bottcher, A.; Niehus, H. *Phys. Rev. B* **1999**, *60*, 14 396. (b) Bottcher, A.; Conrad, H. *J. Chem. Phys.* **2000**, *112*, 4779.

(25) (a) Over, H.; Kim, Y. D.; Seitsonen, A. P.; Wendt, S.; Lundgren, E.; Schmid, M.; Varga, P.; Morgante, A.; Ertl, G. *Science* **2000**, *287*, 1474. (b) Schwegmann, S.; Seitsonen, A. P.; Renzi, V. D.; Dietrich, H.; Bludau, H.; Gierer, M.; Over, H.; Jacobi, K.; Scheffler, M.; Ertl, G. *Phys. Rev. B 57*, **1998**, 15 487.

(26) You, H.; Zurawski, D. J.; Nagy, Z.; Yonco, R. M. *J. Chem. Phys.* **1994**, *100*, 4699. (b) You, H.; Nagy, Z. *Physica B* **1994**, *198*, 187.

(27) Anastasijević, N. A.; Dimitrijević, Z. M.; Adžić, R. R. *Electrochim. Acta* **1986**, *31*, 1125. (b) Walker, R. C.; Bailes, M.; Peter, L. M. *Electrochim. Acta* **1998**, *44*, 1289.

(28) Prakash, J.; Joachin, H. *Electrochim. Acta* **2000**, *45*, 2289.

(29) Robinson, I. K.; In *Handbook on Synchrotron Radiation*; Moncton, D. E., Brown, G. S., Eds.; North-Holland: Amsterdam, 1991; Vol. 3, p 221.

(30) Toney, M. F.; Howard, J. N.; Richer, J.; Borges, G. L.; Gordon, J. G.; Melroy, O. R.; Yee, D.; Sorensen, L. B. *Phys. Rev. Lett.* **1995**, *75*, 4472.

(31) Faguy, P. W.; Marinković, N. S.; Adžić, R. R. *J. Electroanal. Chem.* **1996**, *407*, 209, and references therein. (b) Savich, W.; Sun, S. G.; Lipkowski, J.; Wieckowski, A. *J. Electroanal. Chem.* **1995**, *388*, 233.

(32) Wang, J.; Ocko, B. M.; Davenport, A. J.; Isaacs, H. S. *Phys. Rev. B* **1992**, *46*, 10 321.

(33) Toney, M. F.; Howard, J. N.; Richer, J.; Borges, G. L.; Gordon, J. G.; Melroy, O. R.; Wiesler, D. G.; Yee, D.; Sorensen, L. B. *Nature* **1994**, *368*, 444.

(34) Wang, J. X.; Robinson, I. K.; DeVilbiss, J. E.; Adžić, R. R. *J. Phys. Chem.* **2000**, *33*, 7951.

(35) Adžić, R. R.; Wang, J. X.; Ocko, B. M.; Magnussen, O. M. *J. Phys. Chem.* **1996**, *100*, 14 721.

(36) Sung, Y.-E.; Thomas, S.; Wieckowski, A. *J. Phys. Chem.* **1995**, *99*, 13 513.

(37) Vitus, C. M.; Davenport, A. J. *J. Electrochem. Soc. 141*, **1994**, 1291. (b) unpublished results of X-ray scattering study.